Electronic supplementary information

Bioinspired interface design modulates pathogen and immunocyte responses in biomaterials-centered infection combination therapy†

Jinhua Li,‡[ab] Wei Liu,‡[c] David Kilian,[a] Xianlong Zhang,*[c] Michael Gelinsky[a] and Paul K. Chu*[b]

[a] *Centre for Translational Bone, Joint and Soft Tissue Research, University Hospital and Faculty of Medicine Carl Gustav Carus, Technische Universität Dresden, Fetscherstraße 74, Dresden 01307, Germany*

[b] *Department of Physics and Department of Materials Science and Engineering, City University of Hong Kong, Tat Chee Avenue, Kowloon, Hong Kong, China. E-mail: paul.chu@cityu.edu.hk*

[c] *Department of Orthopaedics, Shanghai Jiao Tong University Affiliated Sixth People's Hospital, Shanghai Jiao Tong University, Shanghai 200233, China. E-mail: xlzhang_joint@163.com*

† Electronic supplementary information (ESI) available. Details on the experimental procedures, supplementary figures (Figure S1 ~ Figure S34), tables (Table S1 ~ Table S5), and references are provided in the ESI.

‡ These authors contributed equally to this work.

Contents

Supplementary Introduction

Biomaterials have been widely applied in orthopedics and traumatology.[1-3] However, biomaterials-centered infection is becoming a formidable and recalcitrant complication that demands repeated surgery, expensive therapy and extended hospitalization,[4] and has an average incidence of 2%~5% in orthopedics in the recent decade.[5] Bacteria naturally form biofilms on native or artificial surfaces.[6] Bacterial biofilms contaminate medical devices, which are the common cause of persistent infections.[7] Mature biofilms possess stubborn resistance against wide varieties of antibacterial therapies, which are usually difficult and costly and even frequently impossible in medical system.[8] Apparently, it is more efficient to prevent rather than treat bacterial biofilm formation, and with this concept, various meaningful approaches have been introduced to enhance the anti-biofilm and anti-infection property of biomaterials by adopting surface functionalization method.[9, 10] For example, administration of prophylactic antibiotics has been proven to prevent bacterial infections after implantation.[9] Nevertheless, once mature biofilms have developed, bacteria will show less respond to local administration of antibiotics,[11] and increasing concerns focus on antibiotic resistance.[12] Meanwhile, antibiotics may impair immune function[13, 14] and induce oxidative damage in mammalian cells.[15] As such, there is an urgent need for alternative anti-infectious strategies without concerns about antibiotic resistance. Other favorable methods include nanomaterial-based "antibiotics"[16, 17], polycationic coatings[18] and quorum-sensing-inhibitor-modified surfaces[19]. In this regard, it is highly desirable to develop new strategies with ease and reliability to reduce biomaterials-centered infections.

Experimental Section

Sample Preparation

Metallic titanium foils (99.95% purity) were cut into square plates with dimensions of 10 mm × 10 mm × 1 mm and 20 mm × 20 mm × 1 mm, mechanically polished (by manufacturer), ultrasonically cleaned in acetone, alcohol and deionized water, and then dried in air for further use. In the animal test, titanium rods with diameter of 1.5 mm and length of 20 mm were used. Surface coatings were prepared on substrate by plasma electrolytic oxidation (PEO; Plasma Technology Ltd) in a series of designed electrolytes, which were listed in Table S1. After that, all the samples were boiled in deionized water for 10 min to eliminate residual sodium ions. The final samples were named as "TiO_2:Co-0", " TiO_2:Co-0.5", " TiO_2:Co-1", " TiO_2:Co-2", and "TiO_2:Co-4", respectively.

Sample Characterization

The surface topographies of samples were examined by field-emission scanning electron microscopy (SEM; LEO 1530, Germany). The crystallinity of surface coatings was studied by X-ray diffractometer (XRD; Rigaku Ultima IV, Japan) using Cu Kα (λ=1.541 Å) source in the range of 2θ = 20º~90º with glancing angle of 1º. Phase identification was performed with the help of the JCPDS database. The surface chemical compositions and chemical states were analyzed by X-ray photoelectron spectroscopy (XPS; Physical Electronics PHI 5802) using Al Kα source (1486.6 eV). Ultraviolet photoelectron spectroscopy (UPS; Thermo Scientific Escalab 250Xi, US) measurement was carried out on an ultraviolet photoelectron spectrometer. The valance band (VB) spectra were measured with a monochromatic He I light source (21.2 eV) and a VG Scienta R4000 analyzer. A sample bias of −5 V was applied to

observe the secondary electron cutoff (SEC). The work function (ϕ) can be determined by the difference between the photon energy and the binding energy of the secondary cutoff edge.[20]

The optical diffuse reflectance spectra of the various samples were recorded on UV-Vis-NIR spectrophotometer (Model UV-4100, Hitachi Corp.). The diffuse reflectance spectra were converted into equivalent absorption coefficient by Kubelka–Munk function:[21]

$$\alpha = (1 - R)^2/2R \quad (1)$$

$$\alpha h\nu = C_1(h\nu - E_g)^2 \quad (2)$$

$$h\nu = 1240/\lambda \quad (3)$$

where: α is the optical absorption coefficient near absorption edge for indirect interband transition; R is the reflectance of semiconductor; C_1 is the constant for indirect transition; $h\nu$ is photon energy; E_g is indirect bandgap energy (eV); λ is wavelength (nm).

Ion Release Determination

The coating samples were positioned in 15 ml sterile microcentrifuge tubes containing 10 ml of trypticase soy broth (TSB) or Dulbecco's Modified Eagle's medium (DMEM). Successive static immersion at 37 ºC was conducted for 1, 4 days, 1, 2, 4, 6, and 8 weeks. At the end of each period of incubation, the leachates were collected and the concentrations of cobalt ions released from the coatings were measured by inductively-coupled plasma optical emission spectrometry (ICP-OES; Perkin Elmer, Optima 2100DV).

In Vitro Cell Evaluation

Cell Source and Culture

The rat bone marrow mesenchymal stem cells (rBMSCs) were purchased from the Chinese Academy of Science cell bank and cultured in DMEM supplemented with 10% fetal bovine serum and 1% penicillin/streptomycin. The cells were cultured at 37 °C in a

humidified 5% CO_2 incubator and passaged every 3 days at ~80% confluence. Only the confluent rBMSCs at passages 3~5 were harvested for further study.

Cell Viability

The cellular viability of rBMSCs was assayed by the Cell Counting Kit-8 (CCK-8, Sigma-Aldrich). First, four samples per group were positioned in new 24-well plates. Then, 5×10^4 cells/well were seeded for each sample. After 1 and 3 days of culture, the culture medium was thoroughly removed and 1 ml of fresh medium with 10% CCK-8 was added to each well, followed by 4 h of incubation. Finally, 100 μl of the culture medium was transferred to a new 96-well plate for measuring the absorbance at 450 nm on a microplate reader (DTX 800 Series Multimode Detectors, Beckman Coulter).

Cell Adhesion and Cytoskeleton

To observe the initial cell adhesion and cytoskeleton spread, the rBMSCs of 5×10^4/well were seeded in a 24-well plate for various samples. After 24 h of culture, the cells were rinsed gently with sterile phosphate-buffered saline (PBS, pH 7.4) three times, fixed in 4% paraformaldehyde for 10 min at 4 ℃, and then permeabilized in 0.1% Triton X-100 (v/v) for 30 min. Subsequently, the rBMSCs were stained with rhodamine phalloidin (Sigma-Aldrich) for actin and 4′,6-diamidino-2-phenylindole (DAPI; Sigma-Aldrich) for cell nuclei in darkness at room temperature. The cell nuclei and cytoskeletal actin were observed on a confocal laser scanning microscopy (CLSM; LSM 510 Meta, Zeiss, Germany).

In Vitro Antibacterial Experiment

Bacteria–Biomaterial Culture

Spread Plate Test

Methicillin-resistant *Staphylococcus aureus* (MRSA, ATCC43300), *Staphylococcus epidermidis* (*S. epidermidis*, ATCC 35984), *Escherichia coli* (*E. coli*, ATCC 35218), and *Pseudomonas aeruginosa* (*P. aeruginosa*, ATCC 27853) were used to evaluate the in vitro antimicrobial effect of the various coating samples (for comparison and analysis, TiO_2:Co-4 was also used). After overnight incubation in fresh TSB medium at 37 °C, 500 μl of bacteria solution (~10^6 CFU/ml) was inoculated into 24-well plates containing the samples (1 cm × 1 cm, four per group), followed by overnight incubation at 37 °C. The number of planktonic bacteria in the original TSB medium was counted using the spread plate method (SPM).[22] Briefly, 100 μl of diluted bacterial suspension was evenly spread on the sheep blood agar (SBA) and recultivated at 37 °C overnight before capturing representative photographs. For counting the number of adherent bacteria, the overnight samples were taken out by sterile forceps and rinsed gently with fresh PBS to dislodge the non-adherent bacteria. Then each sample was positioned in 1 ml of fresh PBS and received 5 min of ultrasonic vibration (150 W, B3500S-MT, Branson Ultrasonics Co., Shanghai) and 2 min of vortex mixing (Vortex Genie 2, Scientific Industries, Bohemia, NY) to drive out the adherent bacteria. The amount of viable bacteria in the suspension was counted using the SPM. The bacterial colonies on SBA were counted according to the National Standard of China GB/T 4789.2 protocol. The expression of $\log_{10}$CFU/ml was adopted to indicate the antimicrobial activity of the various coating samples against planktonic bacteria and sessile bacteria.

Bacterial Biofilm Formation Evaluation Using CLSM and SEM

The Live/Dead BacLight Bacterial Viability Kit (L13152, Invitrogen) was used to visualize the bacterial viability and biofilm formation. After overnight culture, the samples containing bacteria were rinsed gently three times with sterile PBS in a new 24-well plate. Propidium iodide (PI, red fluorescent dye for dead bacteria) and SYTO 9 (green fluorescent dye for live bacteria) were mixed together prior to use. 500 μl of dye mixture was added into

each well at room temperature, followed by 15 min of staining in darkness. Afterwards, the stained samples were observed on the CLSM. All the operations strictly followed the manufacturer's instruction. For the SEM observation, first bacteria were cultured on various samples as above, followed by 4 h of fixing with 2.5% glutaraldehyde at 4 °C. Then the samples were dehydrated successively using a graded ethanol series (50, 70, 80, 90, 95, and 100 v/v%) for 10 min each in a new 24-well plate. Prior to SEM observation, the samples were freeze dried and platinum coated.

Analysis of Biofilm-Related Genes Using qRT-PCR

Biofilm-related genes were analyzed using the quantitative real-time polymerase chain reaction (qRT-PCR). The MRSA was used for the *fnbA* and *fnbB* gene expression assay, and the *S. epidermidis* was used for the *icaA* and *icaR* gene expression assay. 2 ml of bacterial suspension was added to each well containing the coating sample (2 cm × 2 cm) in 6-well plate and statically cultured at 37 ºC overnight. Then the bacteria were collected and pelleted by 5 min of centrifugation at 10,000 g, followed by being re-suspended in 1 ml of PBS containing 100 mg/ml of lysostaphin (Sigma) and then 10 min of incubation at 37 ºC.[23] The total RNA was extracted using the RNeasy Mini Kit (Qiagen, Germany). Afterwards, 1 μg of the total RNA was reverse transcribed to the complementary DNA (cDNA) through the PrimeScript RT reagent Kit (Takara). Finally, the qRT-PCR analysis was conducted on a Bio-Rad C1000 system through SYBR Premix Ex Taq II (Takara). The primers relevant to the target genes are synthesized commercially and presented in Table S5. The expression levels of *fnbA*, *fnbB*, *icaA,* and *icaR* were assayed and normalized to that of the internal standard gene 16S rRNA. The quantification of the expression levels of the target genes was ground on the cycle threshold value of each sample that was computed through the average of three replicate measurements.[23, 24]

Gas Chromatography–Mass Spectrometry (GC-MS) Analysis

After culturing the MRSA bacteria on the samples overnight, the gas above the culture media was collected and its composition was analyzed on a gas chromatography–mass spectrometry (GC-MS) instrument.

Rat Implant-Related Osteomyelitis Model

The protocols for the animal experiments were approved by the Animal Care Committee of Shanghai Jiao Tong University Affiliated Sixth People's Hospital. Thirty-six specific-pathogen-free Sprague Dawley rats were utilized in the experiment (9 rats per group for TiO_2:Co-0, TiO_2:Co-0.5, TiO_2:Co-1, and TiO_2:Co-2). The MRSA was used to establish the rat femoral osteomyelitis. All the surgical procedures were conducted under aseptic conditions. The anesthesia was carried out through the rat intraperitoneal injection of 3% pentobarbital sodium. The left knees were shaved and sterilized with the povidone iodine. Then an incision was made layer by layer using the medial parapatellar approach. Aftwewards, the femoral condyle was exposed and a channel was created in the medullary cavity using a Kirschner wire (1.5 mm diameter). Then 100 μl MRSA in sterile PBS (10^6 CFU/ml) was injected into the channel in the femur medullary cavity. Lastly, one implant (1.5 mm diameter, 20 mm length) was inserted and the incision was closed carefully. The rats were raised in ventilated rooms post surgery and they were allowed to drink and eat freely. The administration of antibiotics was forbidden during the experiment.

Radiographic Assessment

At 0, 2, and 4 weeks post surgery, the radiographs of the rat femurs were captured. Four weeks after the surgery, the rats were euthanized with 3% pentobarbital sodium for the micro-CT scanning (Skyscan 1176, Bruker Micro-CT, Germany). The rat femurs were aseptically obtained and subjected to the high resolution micro-CT scanning. The coronal sections, the

transverse sections, and the overall 3D images were captured using the software from the manufacturer. The bone volume/total volume (%) and the cortical bone mineral density (BMD) of the rat femurs were analyzed with the manufacturer's software.

Microbiological Evaluation

All the implants in the rat femurs were rooted aseptically after the micro-CT scanning. For analyzing the number of adherent bacteria, the implants were positioned in sterile PBS (5 ml), sonicated for 5 min, and then vibrated to detach all the adhering bacteria. The obtained bacterial solution was diluted serially and the number of adherent bacteria was counted using the SPM. After removing the implants, the rat femurs were weighed, frozen, and ground to bone powders using a sterile bone mill.[25] Afterwards, the bone powders were vortexed adequately in fresh PBS (4 ml) for 2 min. After centrifuging, 100 μl supernatant was used for the SPM to count the number of bacteria in the rat femurs.

Histological Evaluation

The rat femurs with explanted implants were fixed and then decalcified. Afterwards, the femurs were dehydrated in ethanol solution and then embedded in paraffin. With the help of microtome (Leica, Hamburg, Germany), histological sections (~5 μm) were acquired and then stained with hematoxylin and eosin (H&E) and Giemsa.

Mechanical Property Evaluation

The mechanical properties of the various coating samples prior to and after the in vivo experiment were investigated through nanoindentation test using a nano indenter (Agilent, Nano Indenter G200, Santa Clara, CA). The constant value of Poisson ratio was 0.27.

Macrophage–Biomaterial–Bacteria Co-Culture

Cell Source and Culture

The murine RAW264.7 macrophages were purchased from the Chinese Academy of Science cell bank and cultured at 37 °C in DMEM with 10% FBS in a humidified atmosphere. The cells were passaged at ~80% confluence.

Cell Viability

The RAW 264.7 macrophages were seeded on the coating samples at a density of 5×10^4 cells/well in the 24-well plate. After being cultured for 1 and 3 days, the CCK-8 test was performed to evaluate the cellular viability on the samples.

Macrophages Activation on Coating Samples

The immunofluorescence staining was carried out to mark the two phenotypes of activated macrophages: iNOS (green fluorescence, M1 marker) and Arg1 (red fluorescence, M2 marker). The RAW 264.7 macrophages were seeded on the coating samples for 1 and 3 days. At the end of each time point, the RAW 264.7 macrophages were scraped from the samples and allowed to reattach in a new 24-well plate for 30 min. After that, the macrophages were fixed in 4% paraformaldehyde at 4 ℃ for 1 h. Then the macrophages were permeabilized with 0.1% Triton X-100 at room temperature for 30 min, then blocked by 3% BSA for 1 h, followed by being incubated with the primary antibodies for iNOS (1:200, Abcam) and Arg1 (1:200, Abcam) at 4 °C overnight. Subsequently, the secondary antibodies donkey anti-rabbit Alexa Fluor 488 (1:200, Abcam) and donkey anti-mouse Alexa Fluor 594 (1:200, Abcam) were used to bind the primary antibodies in darkness for 2 h. Lastly, the cell nuclei of RAW 264.7 macrophages were stained with the DAPI dye (blue fluorescence) and the images were obtained on a fluorescence microscope (Leica).

Cytokine Secretion on Coating Samples

The concentrations of cytokines including TNF-α, IL-6, IL-10, and IL-4 in the medium secreted by the RAW 264.7 macrophages cultured on the samples were measured using the enzyme-linked immunosorbent assay (ELISA). First, the RAW 264.7 macrophages were cultured on the samples for 1, 2, and 3 days. At the end of each time point, the culture medium was collected and centrifuged. After that, the concentrations of the secreted cytokines in the supernatant were determined using the ELISA kits (Anogen, RayBiotech) according to the instructions provided by the manufacturers. The experiments were repeated three times.

Bacteria Phagocytosis by Macrophages using Fluorescence Staining

First, 1 ml of the MRSA bacterial suspension (10^8 CFU/ml) were stained with 2 μl of the 5(6)-carboxyfluorescein diacetate succinimidyl ester (CFDA-SE, 100 μg/ml) for 30 min in darkness. Then the stained MRSA bacteria suspensions were centrifuged and the CFDA-SE was discarded, followed by being rinsed gently with PBS for further use. Subsequently, the RAW 264.7 macrophages were scraped (2×10^5 cells/ml) from the coating samples after 3 days of culture, and then mixed with 100 μl of the stained MRSA (10^8 CFU/ml) for 90 min. Afterwards, the RAW 264.7 macrophages were centrifuged to eliminate the non-phagocytosed MRSA bacteria in the supernatants, and then rinsed gently with PBS. The RAW 264.7 macrophage suspensions were seeded on the new 24-well plate for 15 min for the cell attachment. After that, the RAW 264.7 macrophages were fixed with 4% paraformaldehyde at 4 ℃ for 30 min, then stained with the phalloidin dye to mark the cytoskeleton, and finally observed on a fluorescence microscope (Leica).

Bacteria Phagocytosis by Macrophages using Spread Plate Method

To evaluate the colony forming unit of the phagocytosed MRSA by the RAW 264.7 macrophages, the phagocytosing RAW 264.7 macrophages were rinsed with 1% Triton X-100 to lyse the macrophages for 15 min. Subsequently, the lysate was diluted, spread on the sheep

blood agar (three times per group), and then cultured at 37 ^{o}C overnight. Finally, the representative CFU images were captured.

Phagocytosis Rate of Macrophages Using Flow Cytometer

The phagocytosis rate of the RAW 264.7 macrophages was analyzed on a flow cytometer (Guava, Millipore, USA). 200 μl of the RAW 264.7 macrophage suspensions (together with the phagocytosed stained MRSA bacteria) were added to the 96-well plate and then examined on the flow cytometer (three times per group).

Neutrophil–Biomaterial–Bacteria Co-Culture

The heparinized human whole blood was collected from healthy adult volunteers. The experiment protocols were approved by the Ethics Committee of Shanghai Jiao Tong University affiliated Sixth People's Hospital and each adult volunteer gave the informed consent before blood drawing. The phagocytosis of the MRSA bacteria by the polymorphonuclear leukocytes (i.e. neutrophils) in venous blood was carried out.[26] Briefly, 200 μl of the MRSA bacteria suspension (10^7 CFU/ml) was mixed gently with 1800 μl of the heparinized whole blood. After being mixed gently, 500 μl of the heparinized blood containing the MRSA bacteria (10^6 CFU/ml) was pipetted gently to the new 24-well plate containing the sterile coating samples, followed by static incubation at 37 °C. At the time point of 0, 30, and 60 min, 3 random blood smears per group were prepared, stained with the Wright-Giemsa dye, and finally observed on an optical microscope.

Statistical Analysis

The statistically significant difference (*P*) among the various groups was measured using the one-way analysis of variance and Tukey's multiple comparison tests on a GraphPad Prism 5 statistical software package. All the data were expressed as mean ± standard deviation. A

value of $P < 0.05$ was considered to be statistically significant and marked as "*", $P < 0.01$ was "**", and $P < 0.001$ was "***".

Supplementary Figures

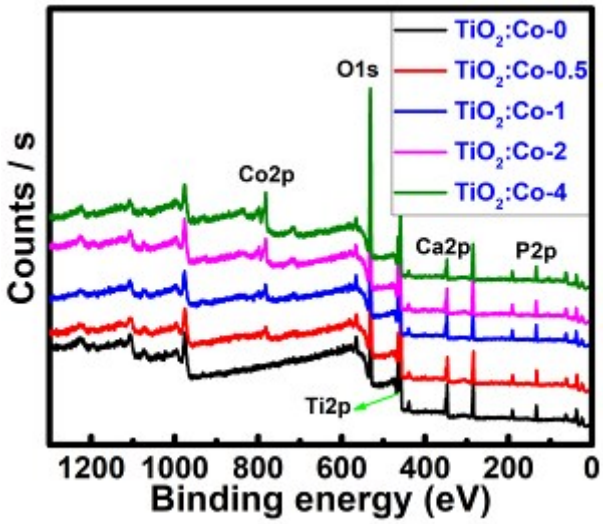

Figure S1. XPS full spectra acquired from the surfaces of the TiO_2:Co-0, TiO_2:Co-0.5, TiO_2:Co-1, TiO_2:Co-2, and TiO_2:Co-4 coatings.

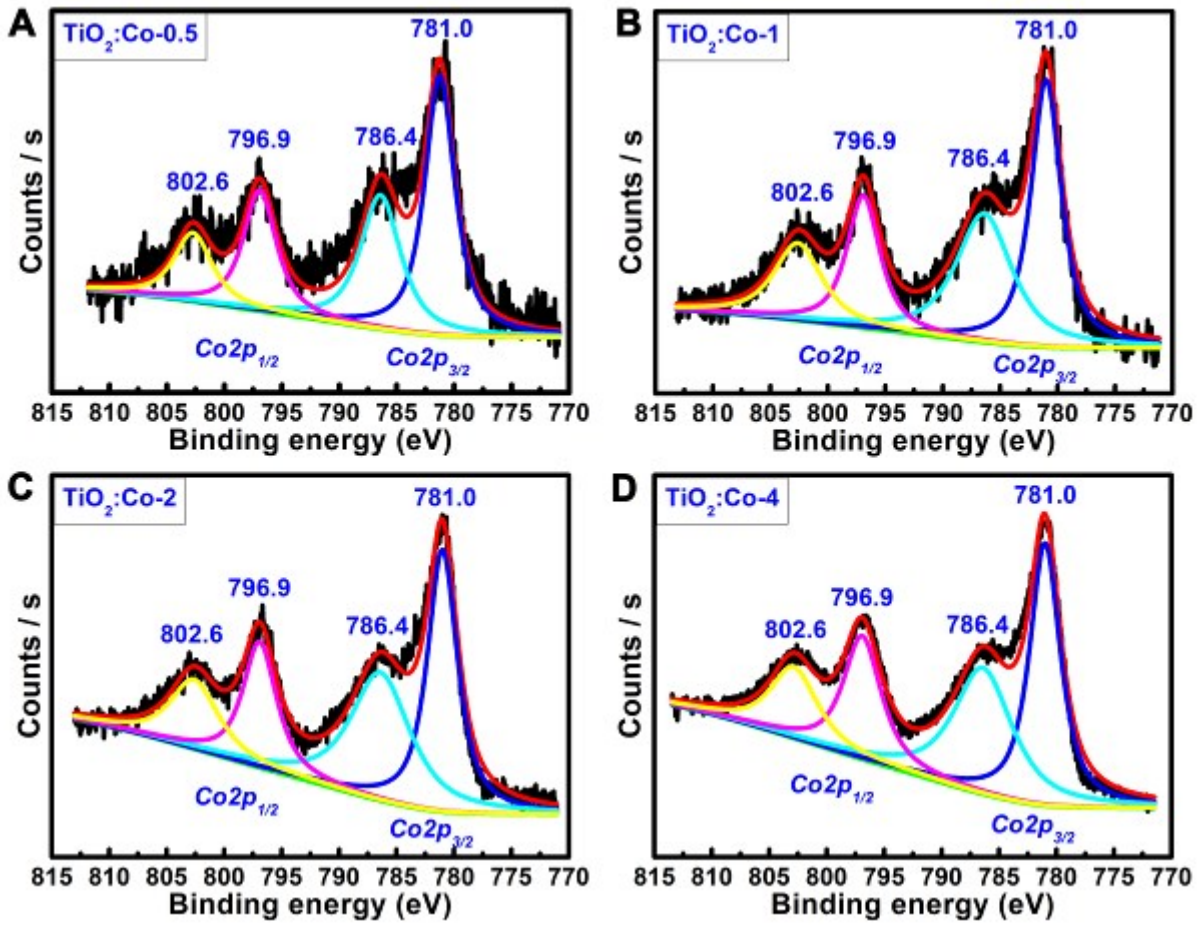

Figure S2. Fitted high resolution Co2p XPS spectra acquired from the surfaces of the TiO_2:Co-0.5 (A), TiO_2:Co-1 (B), TiO_2:Co-2 (C), and TiO_2:Co-4 (D) coatings.

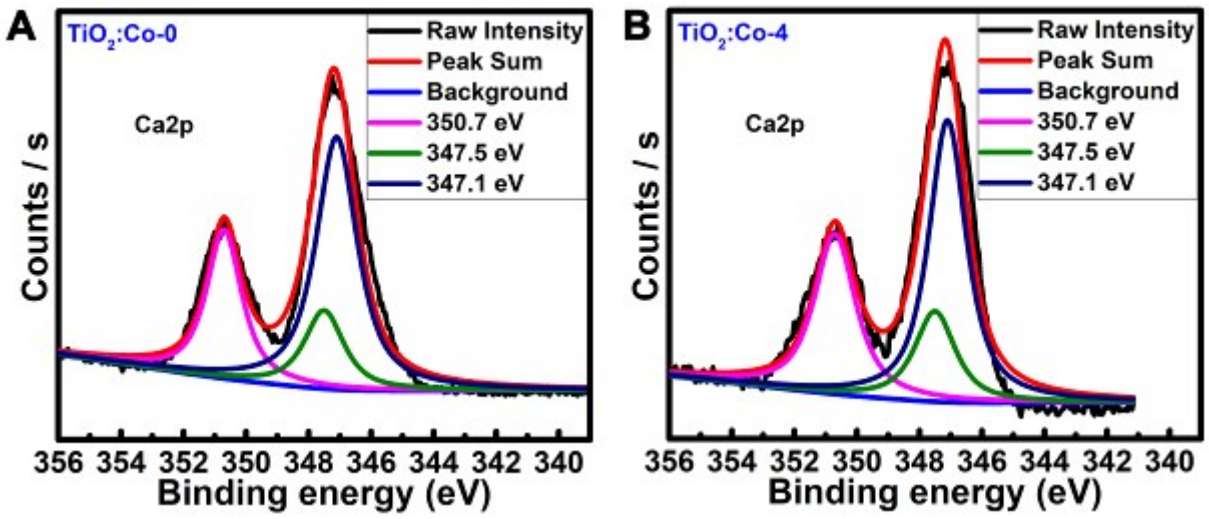

Figure S3. Fitted high resolution Ca2p XPS spectra acquired from the surfaces of the TiO_2:Co-0 (A) and TiO_2:Co-4 (B) coatings.

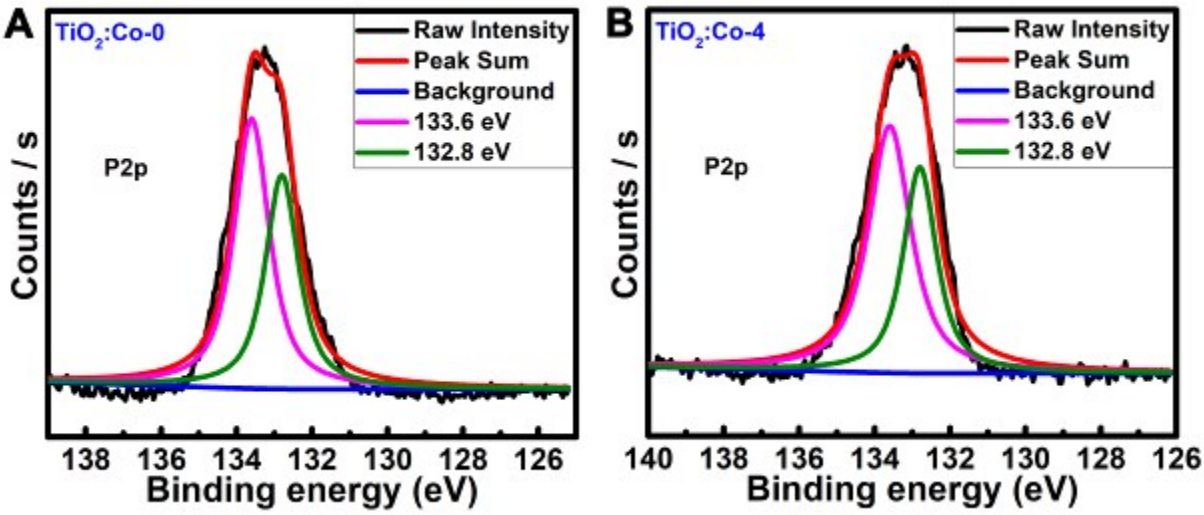

Figure S4. Fitted high resolution P2p XPS spectra acquired from the surfaces of the TiO_2:Co-0 (A) and TiO_2:Co-4 (B) coatings.

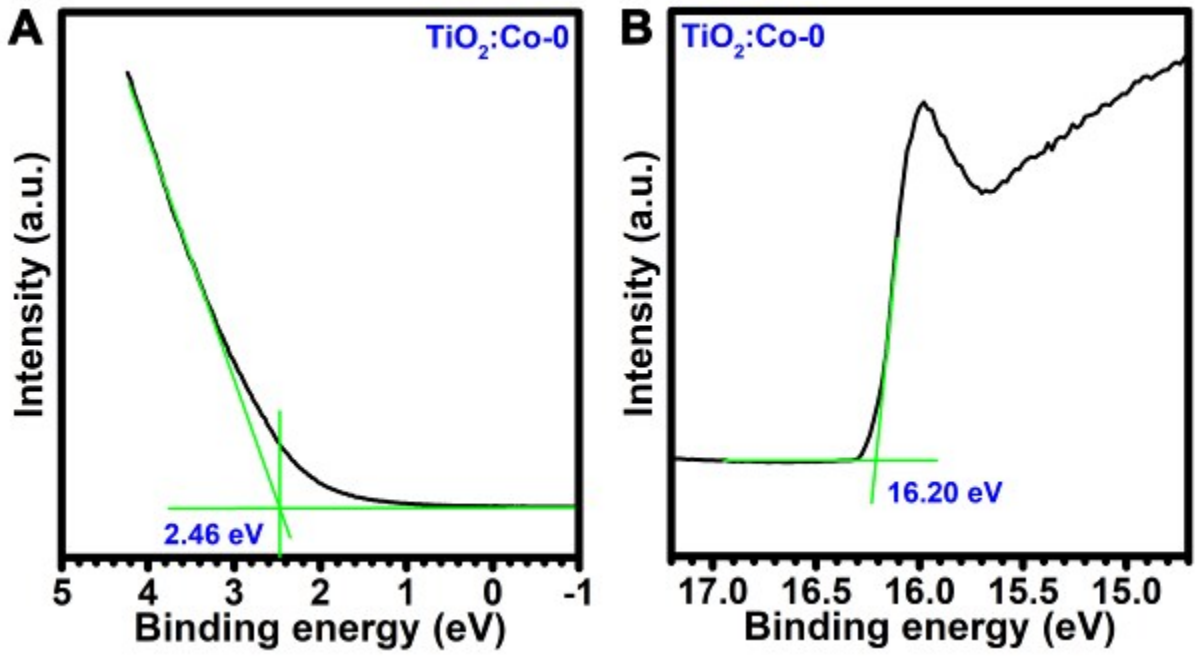

Figure S5. UPS data of the valence band spectrum (A) and secondary electron cutoff (B) acquired from the surface of the TiO_2:Co-0 coating.

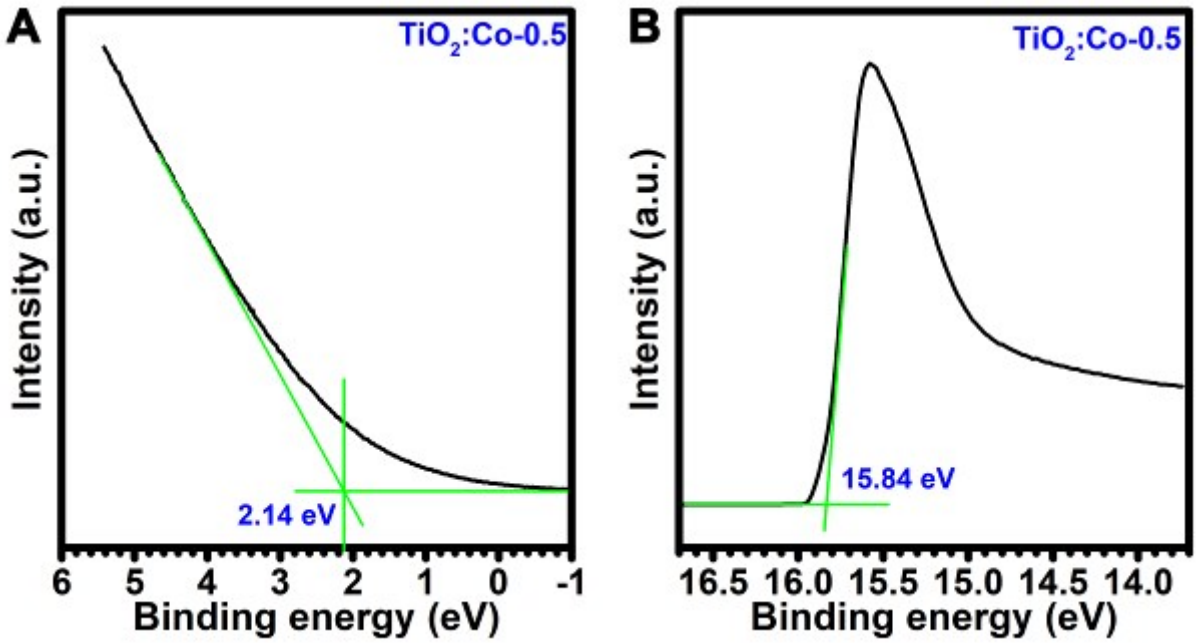

Figure S6. UPS data of the valence band spectrum (A) and secondary electron cutoff (B) acquired from the surface of the TiO_2:Co-0.5 coating.

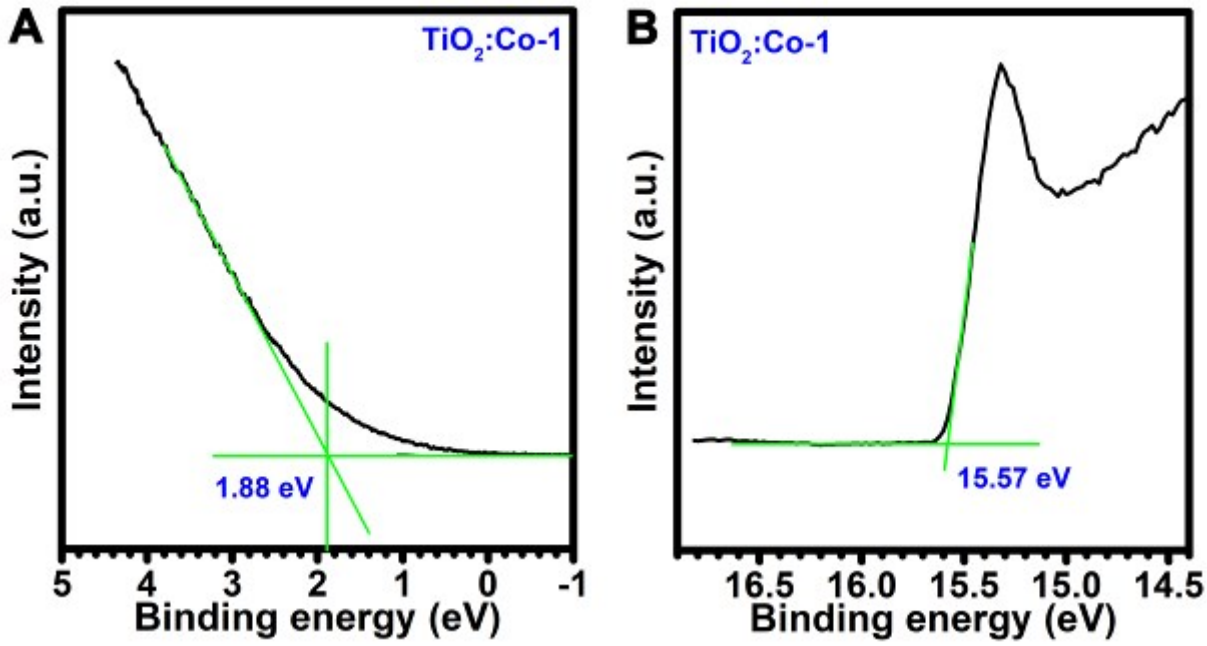

Figure S7. UPS data of the valence band spectrum (A) and secondary electron cutoff (B) acquired from the surface of the TiO_2:Co-1 coating.

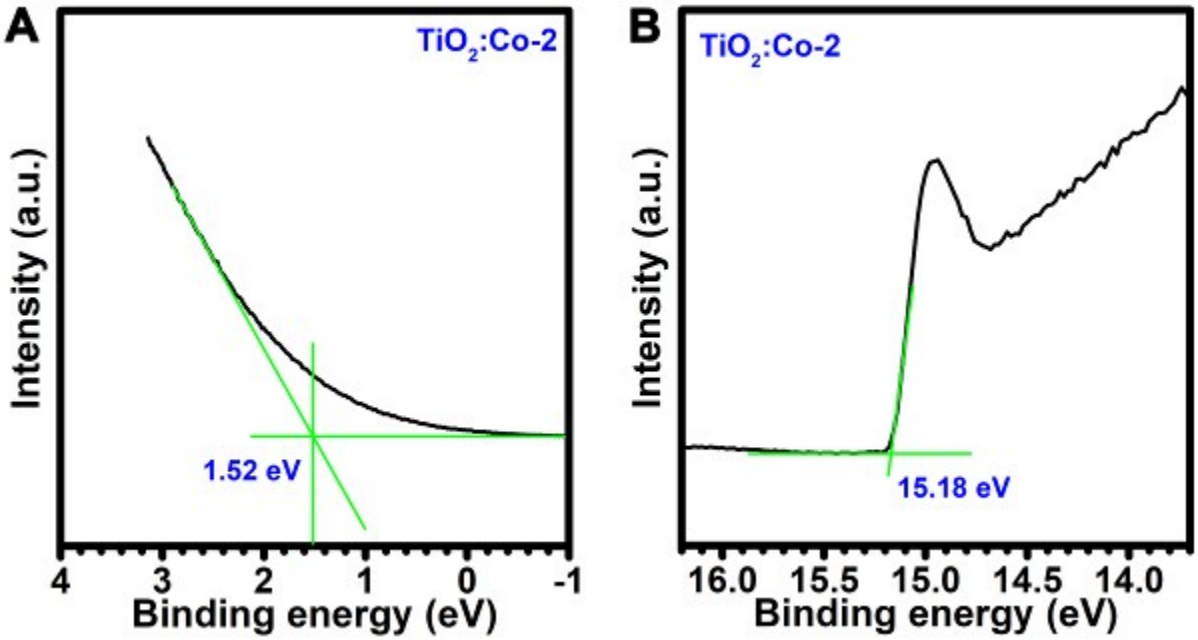

Figure S8. UPS data of the valence band spectrum (A) and secondary electron cutoff (B) acquired from the surface of the TiO_2:Co-2 coating.

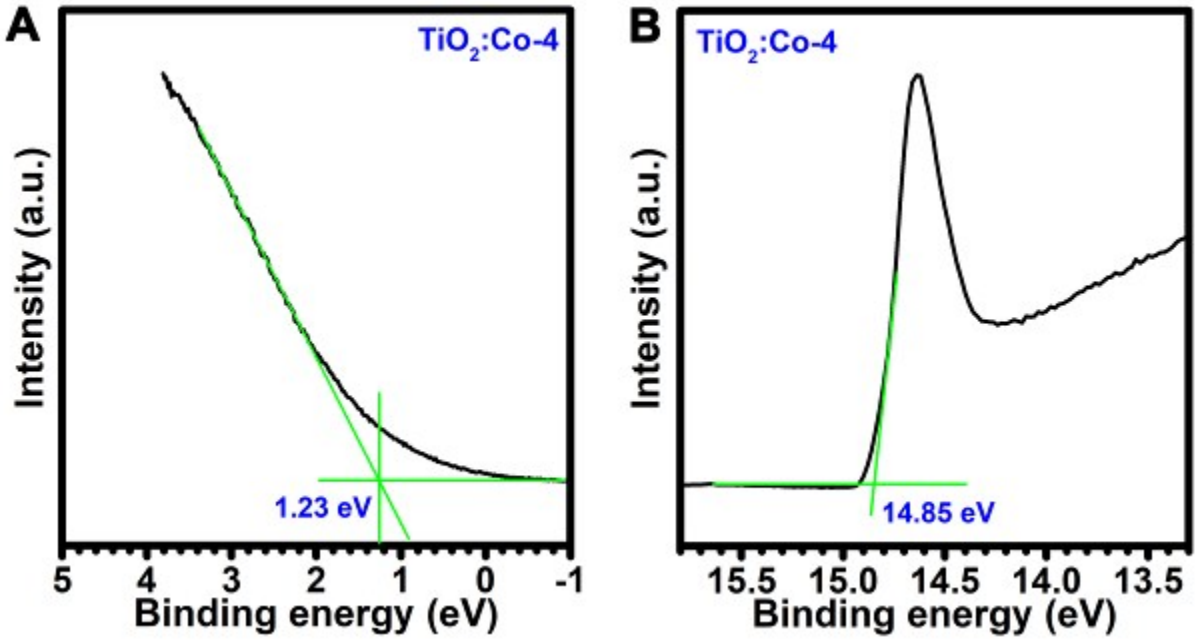

Figure S9. UPS data of the valence band spectrum (A) and secondary electron cutoff (B) acquired from the surface of the TiO_2:Co-4 coating.

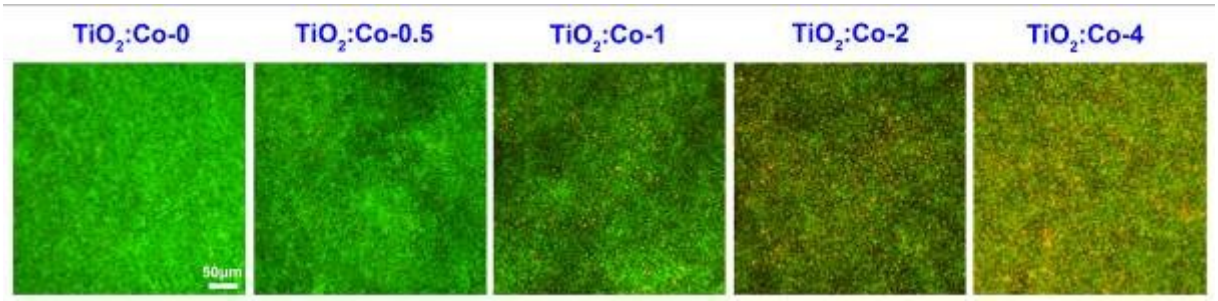

Figure S10. Bacterial viability and biofilm formation of *S. epidermidis* on the coating samples examined by live/dead fluoresence staining method after overnight culture.

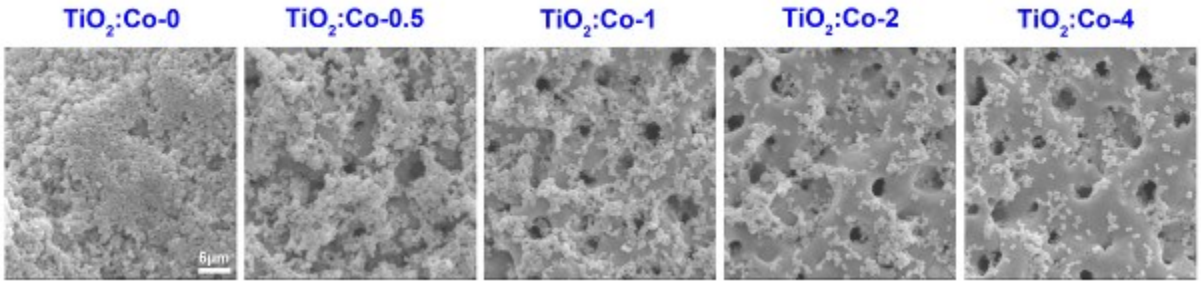

Figure S11. Bacterial viability and biofilm formation of *S. epidermidis* on the coating samples examined by SEM method after overnight culture.

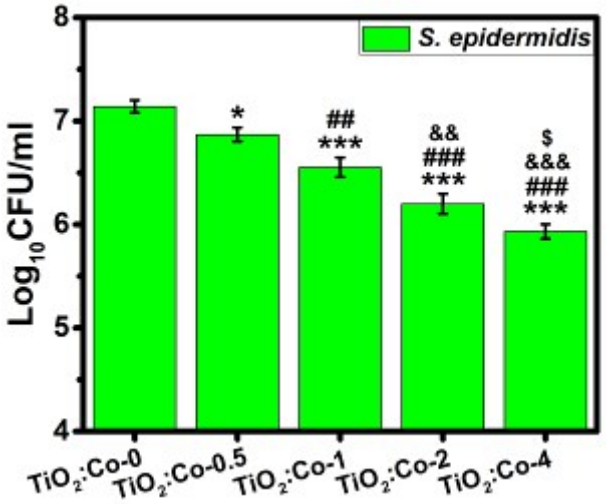

Figure S12. Bacteria colony-forming unit (CFU) of *S. epidermidis* recovered from the coating samples. Signifcant differences for all pairwise comparisons are indicated by the symbols over the bars: *P < 0.05 and ***P < 0.001 vs TiO_2:Co-0; $^{\#\#}$P < 0.01 and $^{\#\#\#}$P < 0.001 vs TiO_2:Co-0.5; $^{\&\&}$P < 0.01 and $^{\&\&\&}$P < 0.001 vs TiO_2:Co-1; $^{\$}$P < 0.05 vs TiO_2:Co-2.

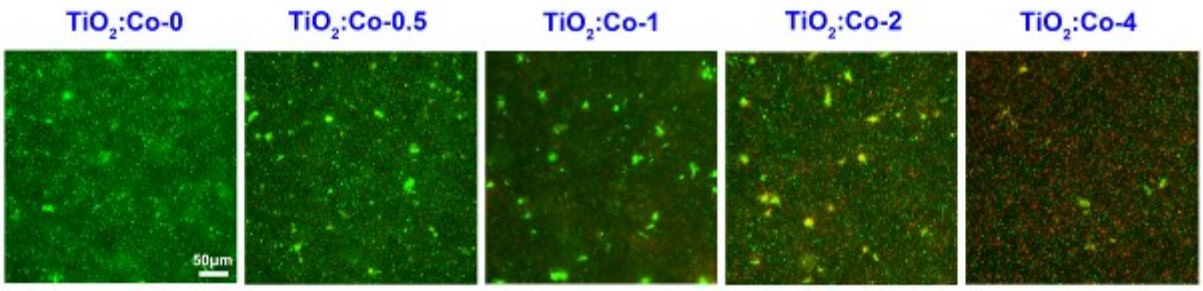

Figure S13. Bacterial viability and biofilm formation of *P. aeruginosa* on the coating samples examined by live/dead fluoresence staining method after overnight culture.

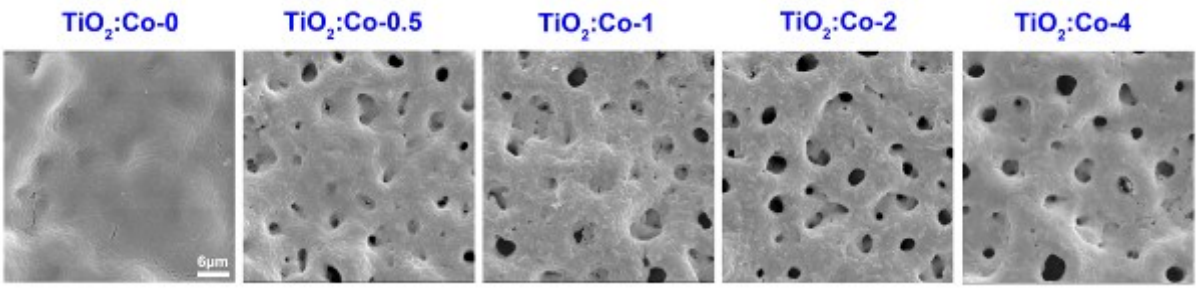

Figure S14. Bacterial viability and biofilm formation of *P. aeruginosa* on the coating samples examined by SEM method after overnight culture.

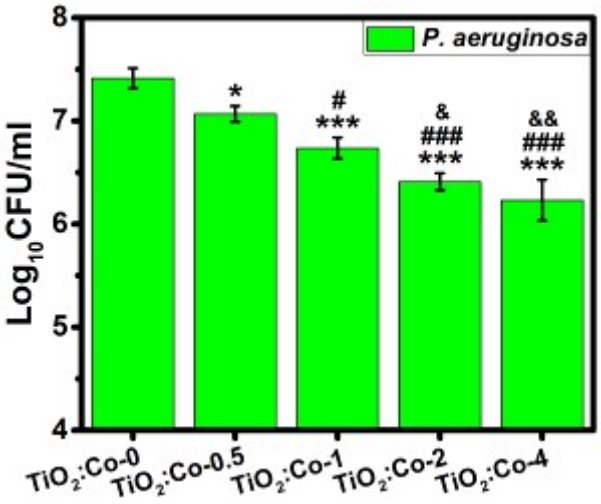

Figure S15. Bacteria colony-forming unit (CFU) of *P. aeruginosa* recovered from the coating samples. Signifcant differences for all pairwise comparisons are indicated by the symbols over the bars: *P < 0.05 and ***P < 0.001 vs TiO_2:Co-0; $^{\#}$P < 0.05 and $^{\#\#\#}$P < 0.001 vs TiO_2:Co-0.5; $^{\&}$P < 0.05 and $^{\&\&}$P < 0.01 vs TiO_2:Co-1.

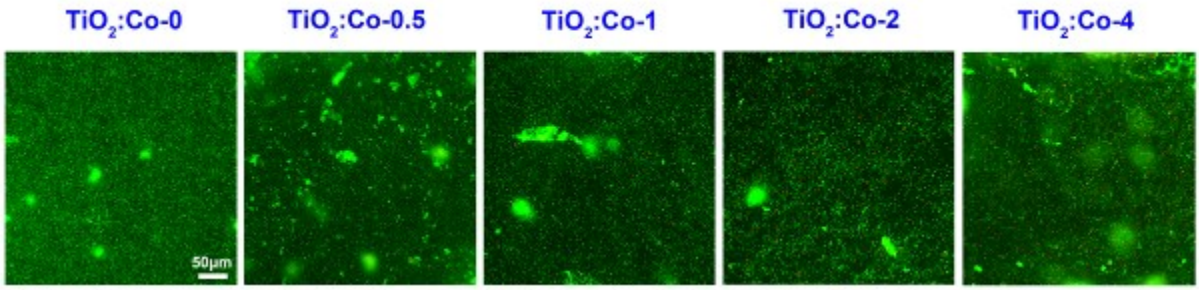

Figure S16. Bacterial viability and biofilm formation of *E. coli* on the coating samples examined by live/dead fluoresence staining method after overnight culture.

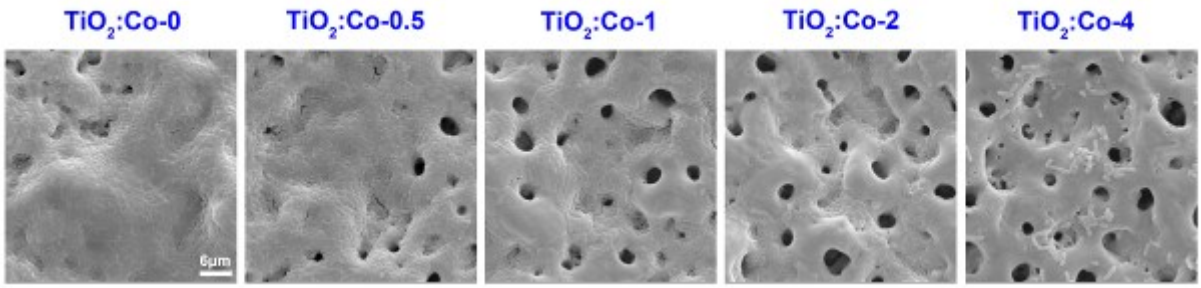

Figure S17. Bacterial viability and biofilm formation of *E. coli* on the coating samples examined by SEM method after overnight culture.

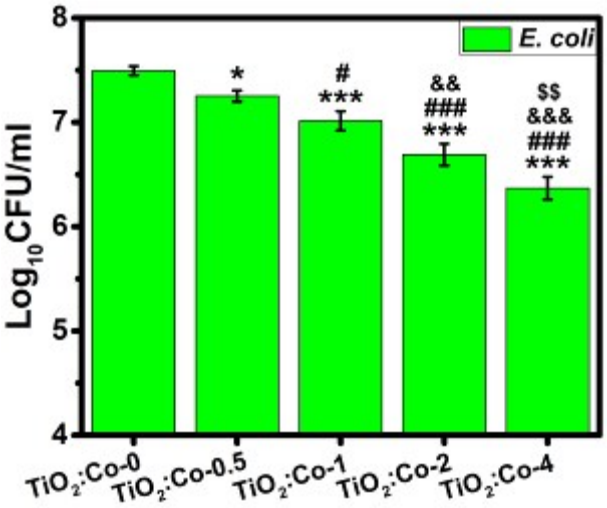

Figure S18. Bacteria colony-forming unit (CFU) of *E. coli* recovered from the coating samples. Signifcant differences for all pairwise comparisons are indicated by the symbols over the bars: *P < 0.05 and ***P < 0.001 vs TiO_2:Co-0; $^{\#}$P < 0.05 and $^{\#\#\#}$P < 0.001 vs TiO_2:Co-0.5; $^{\&\&}$P < 0.01 and $^{\&\&\&}$P < 0.001 vs TiO_2:Co-1; $^{\$\$}$P < 0.01 vs TiO_2:Co-2.

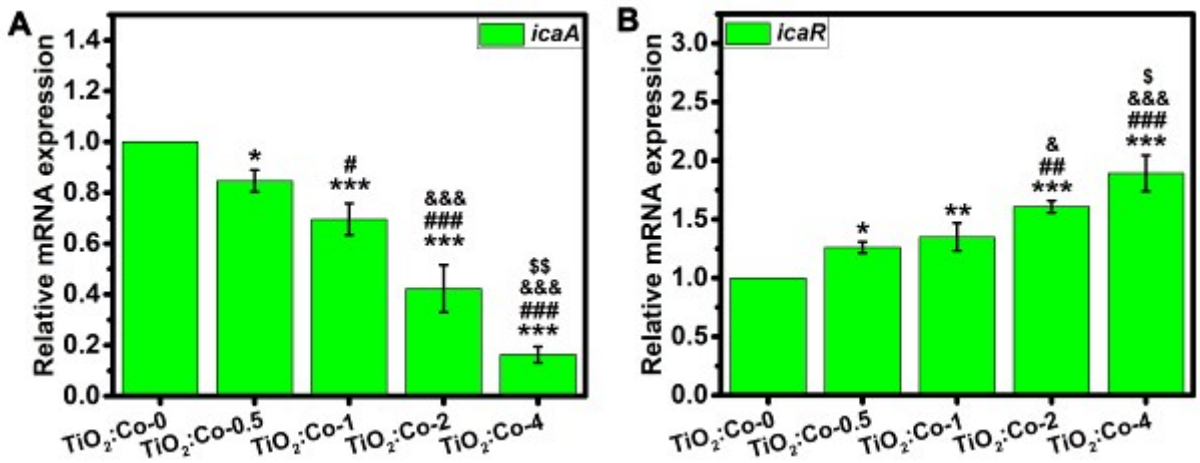

Figure S19. The effect of the coatings on the biofilm genes *icaA* (A) and *icaR* (B) of *S. epidermidis* transcription by qRT-PCR, normalized to the 16S rRNA gene. Signifcant differences for all pairwise comparisons are indicated by the symbols over the bars: *P < 0.05, **P < 0.01, and ***P < 0.001 vs TiO_2:Co-0; $^{\#}$P < 0.05, $^{\#\#}$P < 0.01, and $^{\#\#\#}$P < 0.001 vs TiO_2:Co-0.5; $^{\&}$P < 0.05 and $^{\&\&\&}$P < 0.001 vs TiO_2:Co-1; $^{\$}$P < 0.05 and $^{\$\$}$P < 0.01 vs TiO_2:Co-2.

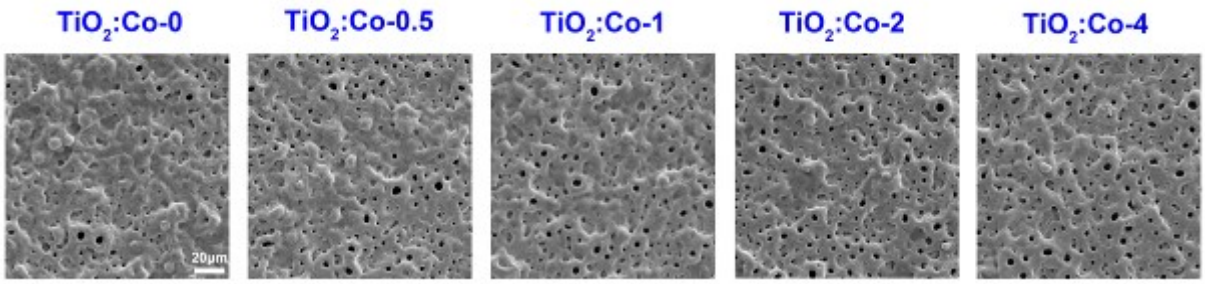

Figure S20. The morphologies of the rBMSCs cultured on the various coating samples for 3 days examined by SEM method.

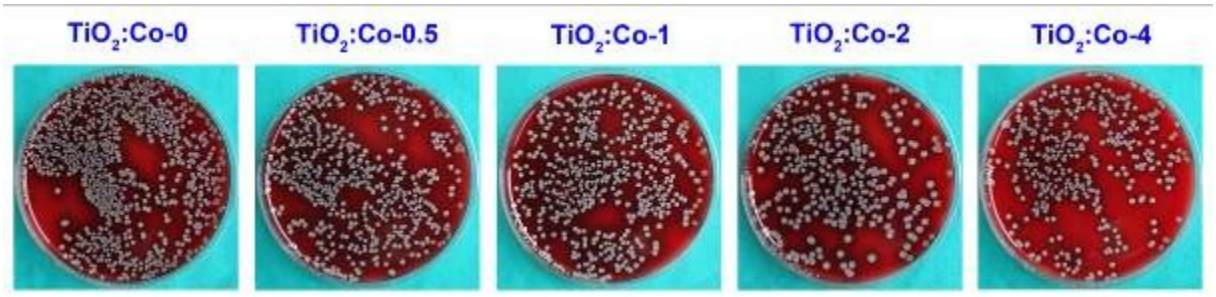

Figure S21. Representative images of bacteria colony-forming unit (CFU) recovered from the planktonic MRSA co-cultured with the samples.

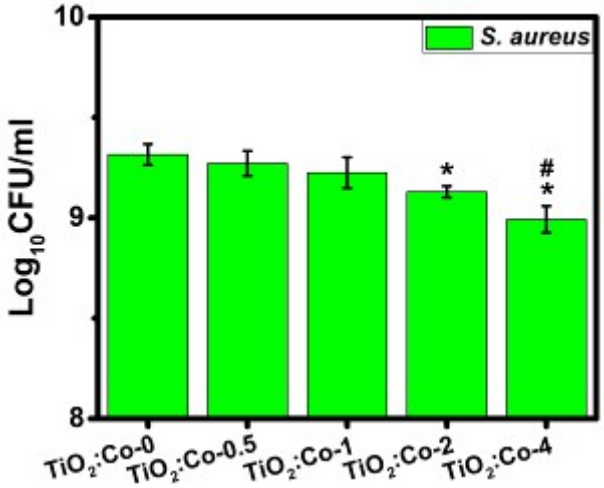

Figure S22. Bacteria colony-forming unit (CFU) recovered from the planktonic MRSA co-cultured with the samples. Signifcant differences for all pairwise comparisons are indicated by the symbols over the bars: *P < 0.05 vs TiO_2:Co-0; $^{\#}$P < 0.05 vs TiO_2:Co-0.5.

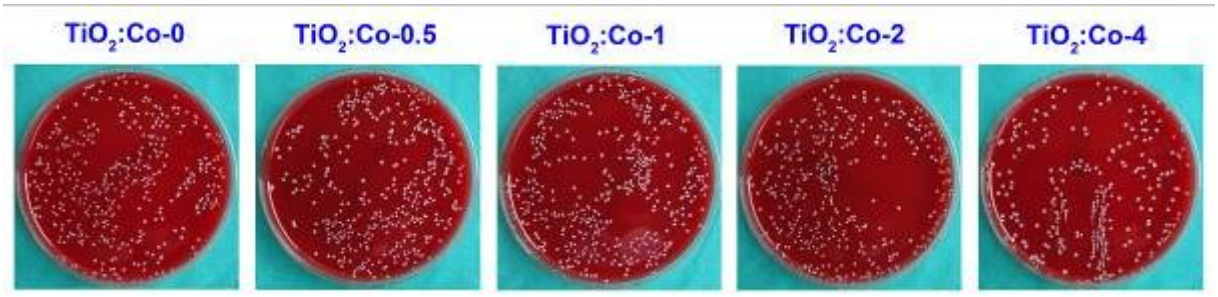

Figure S23. Representative images of bacteria colony-forming unit (CFU) recovered from the planktonic *S. epidermidis* co-cultured with the samples.

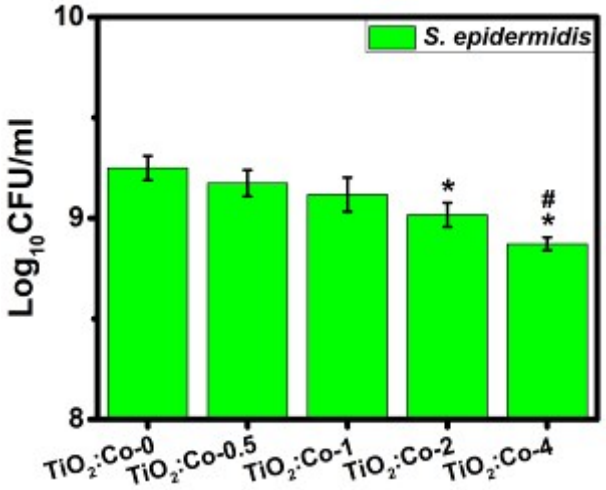

Figure S24. Bacteria colony-forming unit (CFU) recovered from the planktonic *S. epidermidis* co-cultured with the samples. Signifcant differences for all pairwise comparisons are indicated by the symbols over the bars: *P < 0.05 vs TiO_2:Co-0; #P < 0.05 vs TiO_2:Co-0.5.

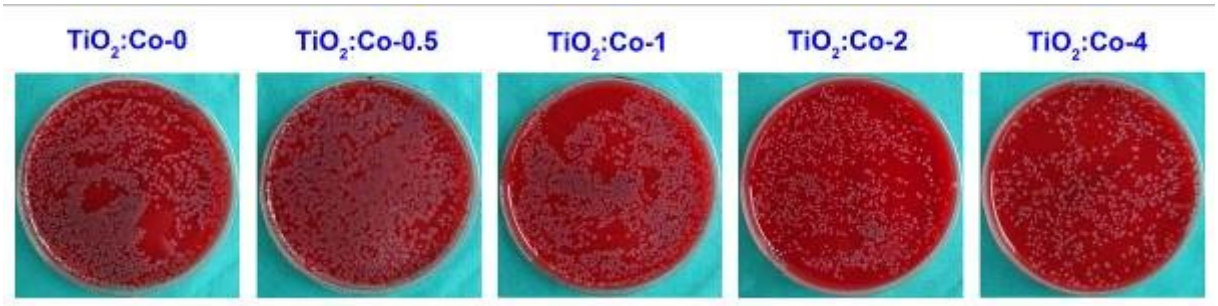

Figure S25. Representative images of bacteria colony-forming unit (CFU) recovered from the planktonic *P. aeruginosa* co-cultured with the samples.

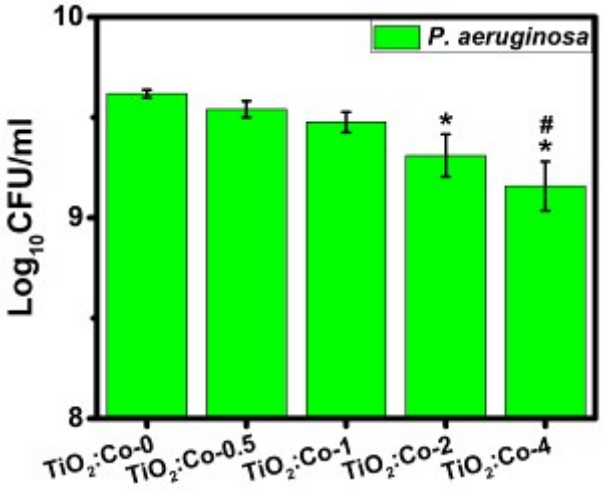

Figure S26. Bacteria colony-forming unit (CFU) recovered from the planktonic *P. aeruginosa* co-cultured with the samples. Signifcant differences for all pairwise comparisons are indicated by the symbols over the bars: *P < 0.05 vs TiO_2:Co-0; #P < 0.05 vs TiO_2:Co-0.5.

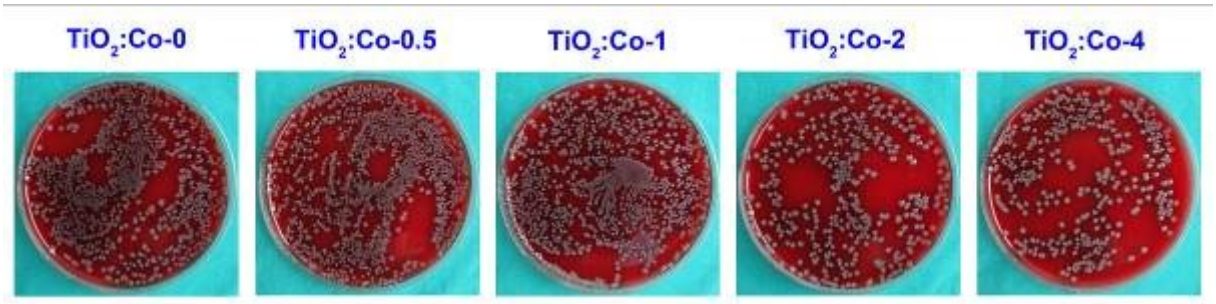

Figure S27. Representative images of bacteria colony-forming unit (CFU) recovered from the planktonic *E. coli* co-cultured with the samples.

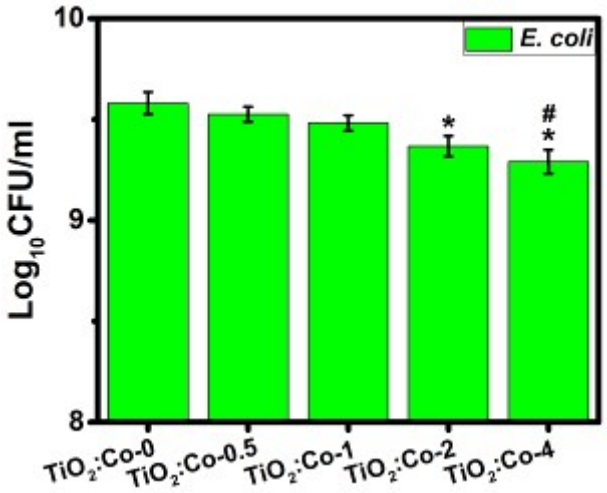

Figure S28. Bacteria colony-forming unit (CFU) recovered from the planktonic *E. coli* co-cultured with the samples. Signifcant differences for all pairwise comparisons are indicated by the symbols over the bars: *P < 0.05 vs TiO_2:Co-0; #P < 0.05 vs TiO_2:Co-0.5.

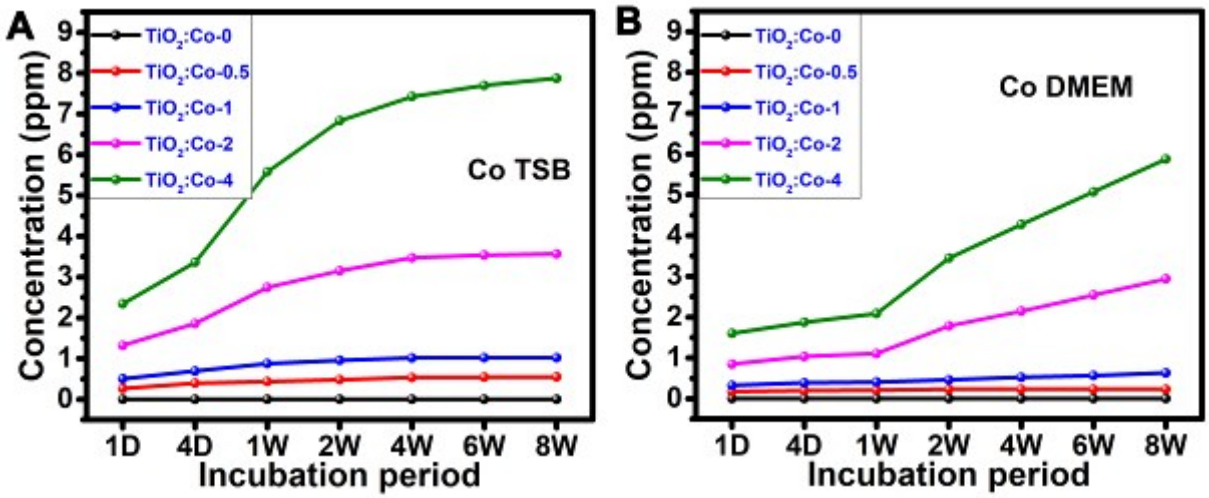

Figure S29. Ion release profiles of Co^{2+} from the coating samples after immersion in TSB (A) and DMEM (B) for 1, 4 days, 1, 2, 4, 6, and 8 weeks measured with ICP-OES.

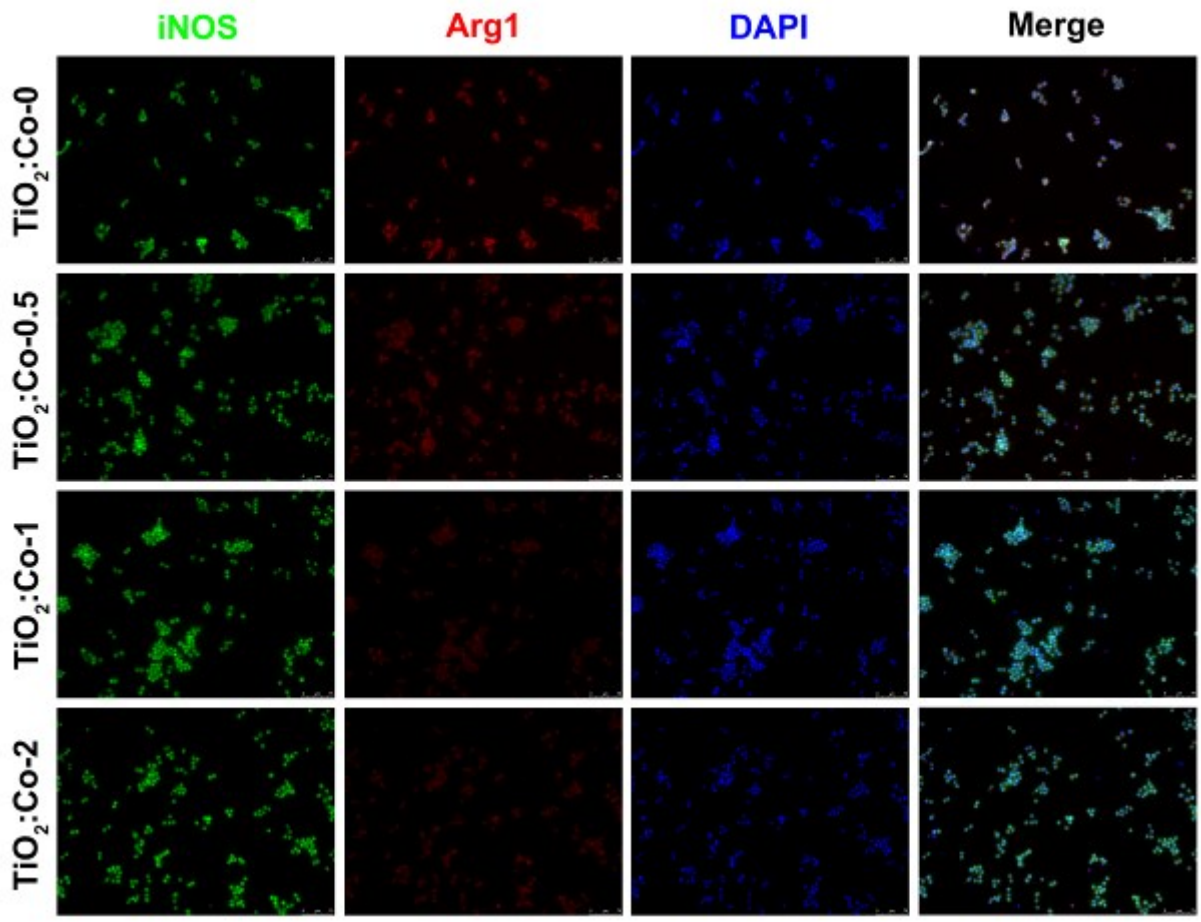

Figure S30. The immunofluorescent staining images of the RAW 264.7 macrophages scratched from the coatings at 1 day post-culture. The green fluorescence shows iNOS positive for M1 phenotype macrophages, the red fluorescence shows Arg1 positive for M2 phenotype macrophages, and the blue fluorescence shows the cell nuclei.

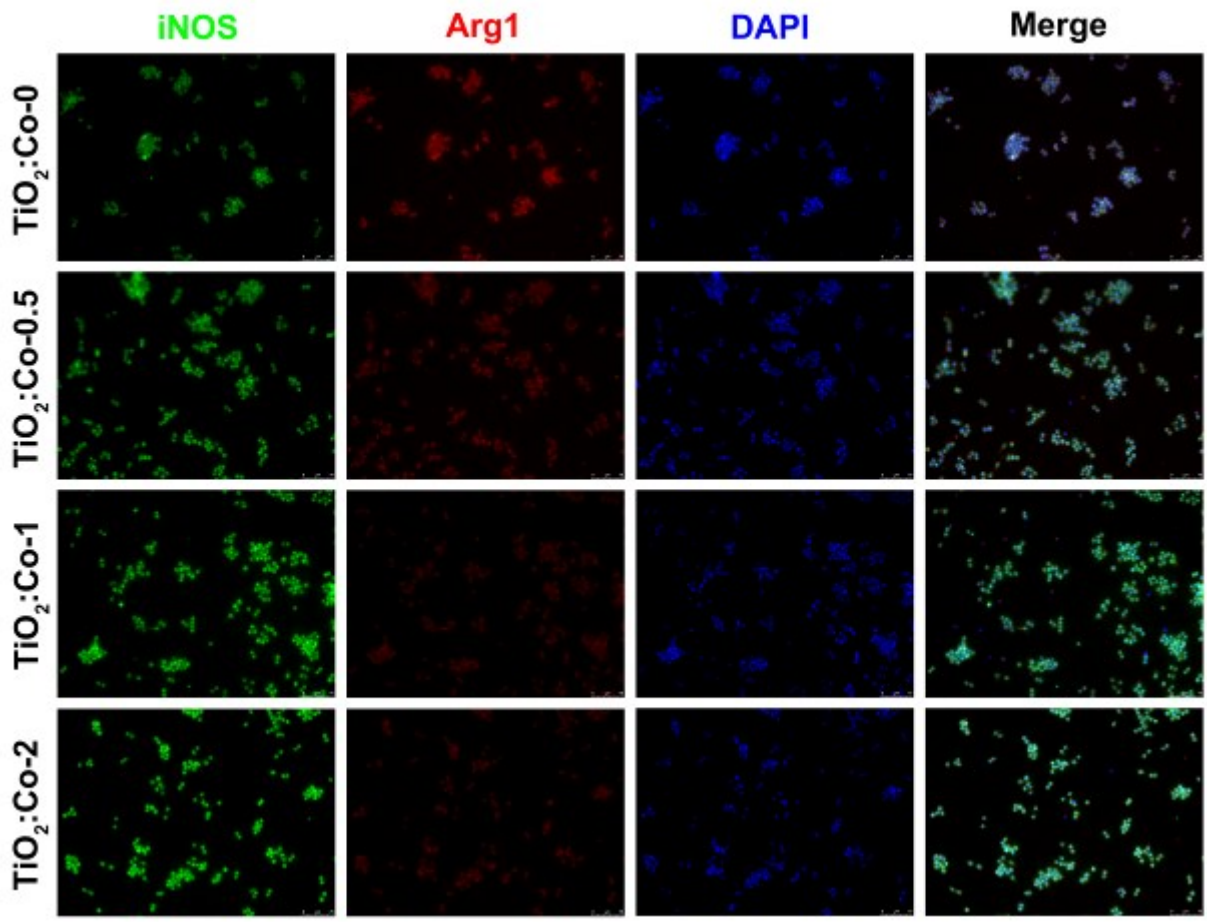

Figure S31. The immunofluorescent staining images of the RAW 264.7 macrophages scratched from the coatings at 3 days post-culture. The green fluorescence shows iNOS positive for M1 phenotype macrophages, the red fluorescence shows Arg1 positive for M2 phenotype macrophages, and the blue fluorescence shows the cell nuclei.

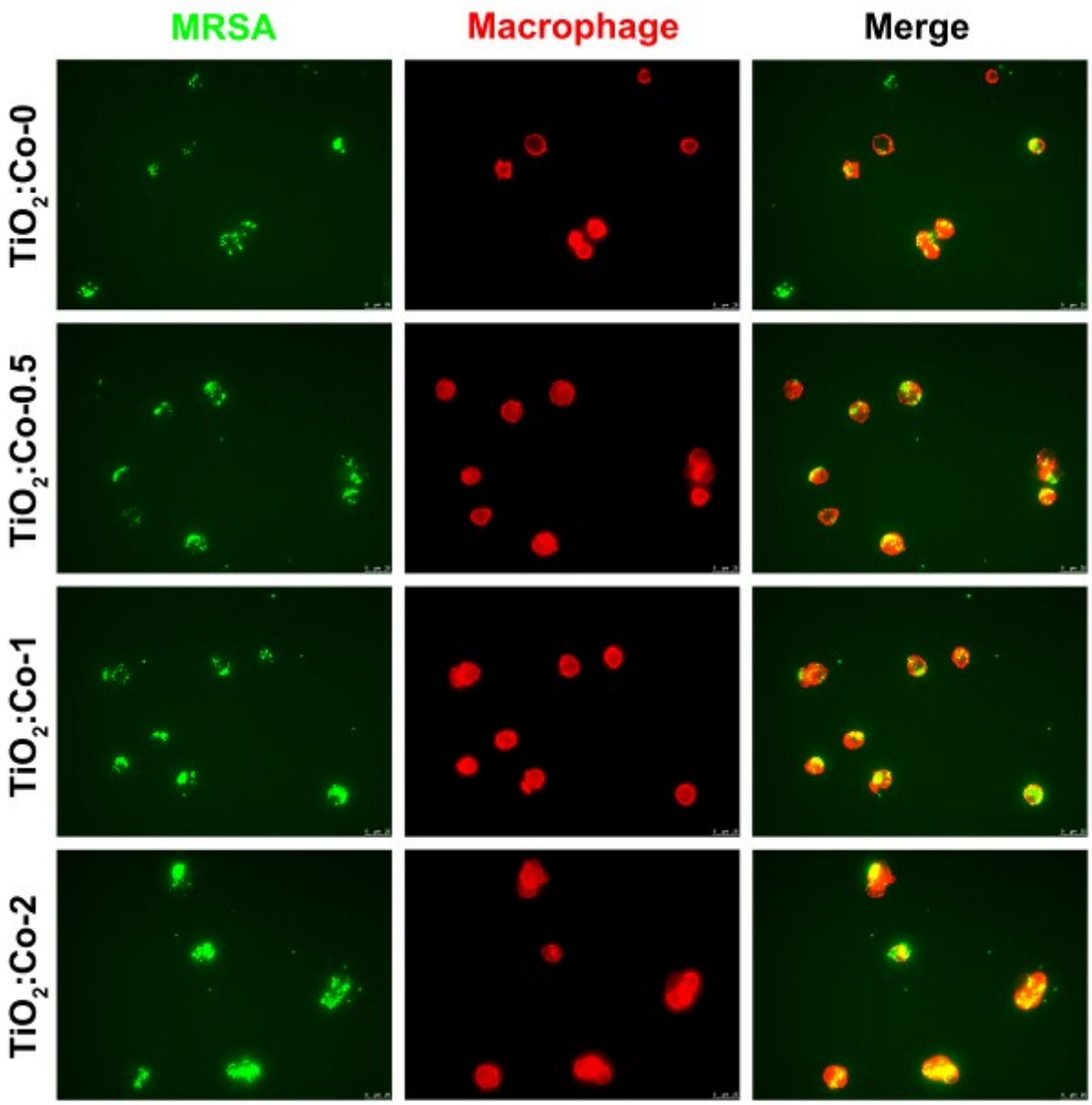

Figure S32. The fluorescence staining images of phagocytosis of MRSA bacteria by the sample-conditioned RAW264.7 macrophages. The green fluorescence shows the phagocytosed bacteria, and the red fluorescence shows the macrophages (cytoskeleton).

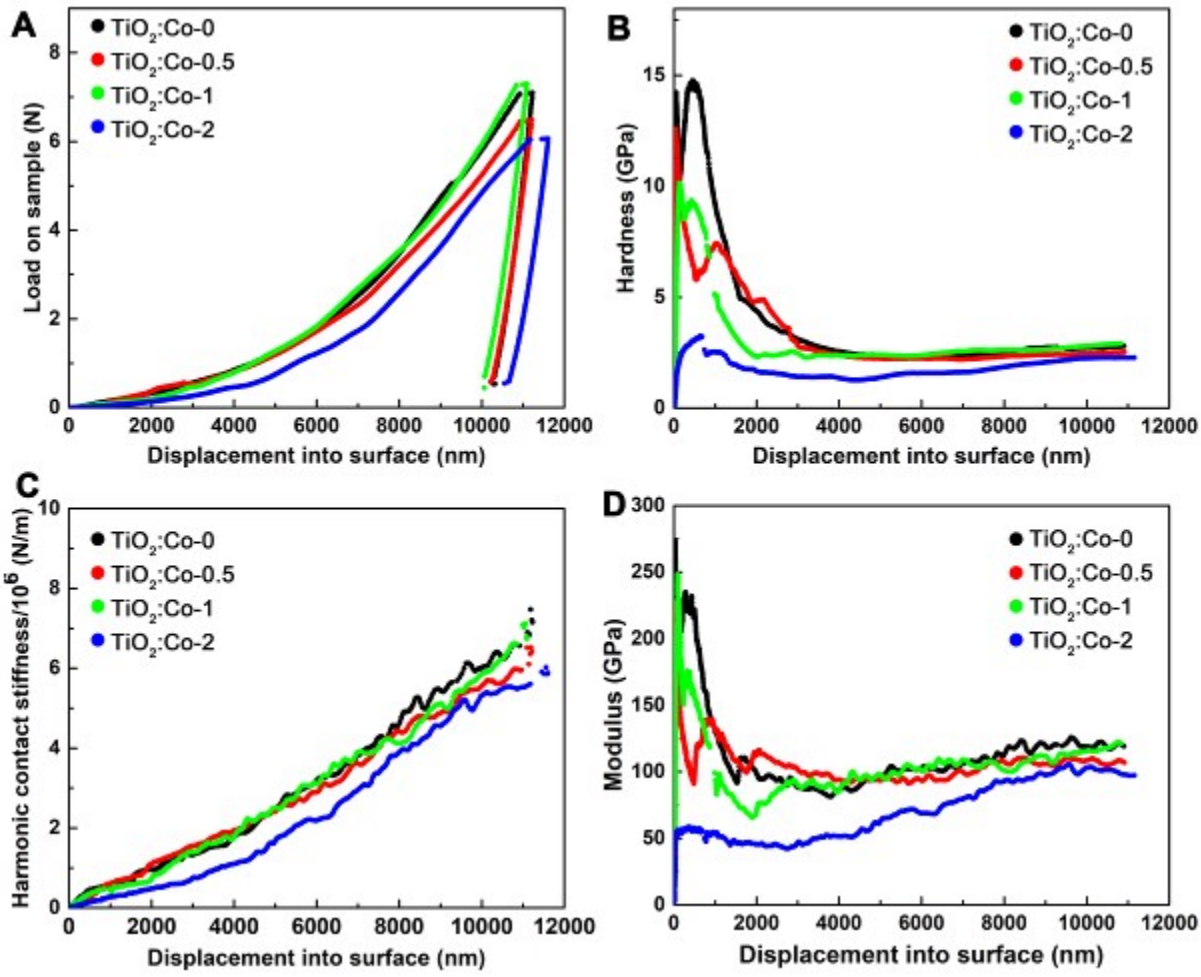

Figure S33. The mechanical properties of the coating samples prior to the in vivo experiment. A) Load–displacement curves. B) Hardness–displacement curves. C) Harmonic contact stiffness–displacement curves. D) Elastic modulus–displacement curves.

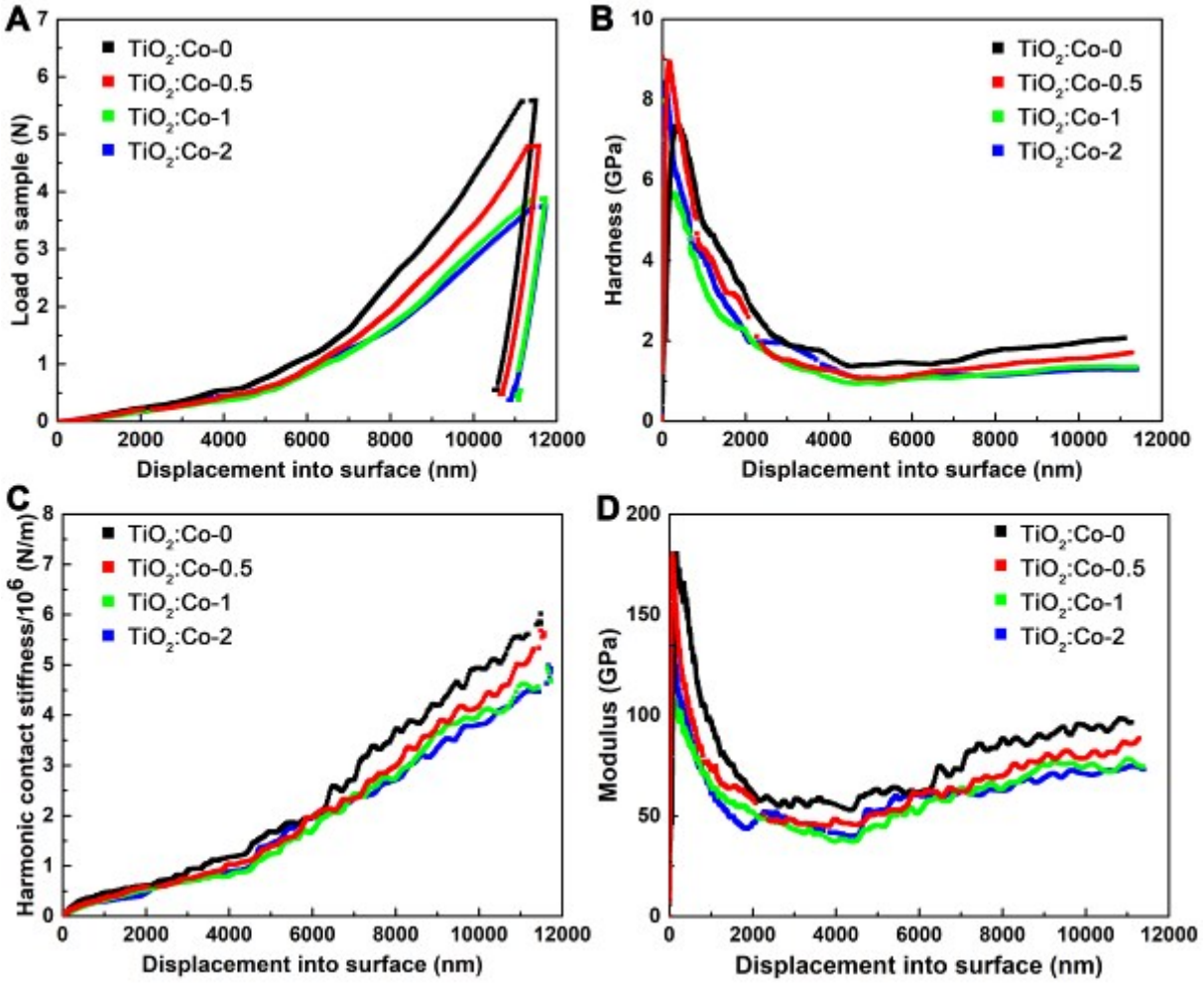

Figure S34. The mechanical properties of the coating samples after the in vivo experiment. A) Load–displacement curves. B) Hardness–displacement curves. C) Harmonic contact stiffness–displacement curves. D) Elastic modulus–displacement curves.

Supplementary Tables

Table S1. Compositions of the various electrolytes applied for plasma electrolytic oxidation treatment.

Sample	Electrolyte composition (M)			
	$C_4H_6O_4Ca \cdot H_2O$	$C_3H_7Na_2O_6P \cdot 5H_2O$	$C_4H_6CoO_4 \cdot 4H_2O$	Co/Ca
TiO_2:Co-0	0.1	0.05	0	0/8
TiO_2:Co-0.5	0.1	0.05	0.00625	0.5/8
TiO_2:Co-1	0.1	0.05	0.0125	1/8
TiO_2:Co-2	0.1	0.05	0.025	2/8
TiO_2:Co-4	0.1	0.05	0.05	4/8

Table S2. Elemental percent content of various samples determined by XPS analysis.

Sample	Elemental contents (at%)				
	O	Ti	Ca	P	Co
TiO_2:Co-0	67.51	15.50	7.16	9.83	0
TiO_2:Co-0.5	66.90	14.54	5.86	10.79	1.91
TiO_2:Co-1	66.92	13.98	5.89	10.76	2.45
TiO_2:Co-2	66.93	13.50	5.31	10.19	4.07
TiO_2:Co-4	67.98	11.75	4.33	9.92	6.03

Table S3. Data for the energy level positions of TiO_2:Co-0, TiO_2:Co-0.5, TiO_2:Co-1, TiO_2:Co-2 and TiO_2:Co-4 coatings.

Coating	Band gap (eV)	Valence band (eV)	Conduction band (eV)	Electron affinity (eV)	Work function (eV)
TiO_2:Co-0	3.10	−7.46	−4.36	4.36	5.00
TiO_2:Co-0.5	2.69	−7.50	−4.81	4.81	5.36
TiO_2:Co-1	2.37	−7.51	−5.14	5.14	5.63
TiO_2:Co-2	1.91	−7.54	−5.63	5.63	6.02
TiO_2:Co-4	1.55	−7.58	−6.03	6.03	6.35

Table S4. The redox potentials for redox couples in the electron transfer system of respiration chain located on bacterial membrane.[27-33]

Half-reaction	Redox couple	Redox potential (E°/V)
$O_2 + 4H^+ + 4e^- \rightarrow 2H_2O$	O_2/H_2O	+0.816
Cytochrome a_3 ox + $e^- \rightarrow$ Cytochrome a_3 red	Cytochrome a_3 ox/red	+0.385
$F_{420} + 2H^+ + 2e^- \rightarrow F_{420}H_2$	$F_{420}/F_{420}H_2$	+0.357
Cytochrome c_1 ox + $e^- \rightarrow$ Cytochrome c_1 red	Cytochrome c_1 ox/red	+0.230
Ubiquinone ox + $e^- \rightarrow$ Ubiquinone red	Ubiquinone ox/red	+0.113
Cytochrome b ox + $e^- \rightarrow$ Cytochrome b red	Cytochrome b ox/red	+0.035
Rubredoxin ox + $e^- \rightarrow$ Rubredoxin red	Rubredoxin ox/red	−0.057
Menaquinone ox + $e^- \rightarrow$ Menaquinone red	Menaquinone ox/red	−0.075
$FMN + 2H^+ + 2e^- \rightarrow FMNH_2$	$FMN^{2+}/FMNH_2$	−0.190
$FAD + 2H^+ + 2e^- \rightarrow FADH_2$	$FAD^{2+}/FADH_2$	−0.220
Cytochrome c_3 ox + $e^- \rightarrow$ Cytochrome c_3 red	Cytochrome c_3 ox/red	−0.290
$NAD + 2H^+ + 2e^- \rightarrow NADH + H^+$	$NAD^+/NADH$	−0.320
$NADP + 2H^+ + 2e^- \rightarrow NADPH + H^+$	$NADP^+/NADPH$	−0.320
Flavodoxin ox + $e^- \rightarrow$ Flavodoxin red	Flavodoxin ox/red	−0.371
Ferredoxin ox + $e^- \rightarrow$ Ferredoxin red	Ferredoxin ox/red	−0.398
$2H^+ + 2e^- \rightarrow H_2$	H^+/H_2	−0.414

[a] pH = 7.0. [b] Abbreviations: F_{420}, coenzyme F_{420}; $F_{420}H_2$, reduced coenzyme F_{420}, quinone oxidoreductase.

Table S5. Primers used in the present study for real-time polymerase chain reaction.

Target gene	Direction	Primer sequence (5'→3')
*ica*A	F	AACAAGTTGAAGGCATCTCC
*ica*A	R	GATGCTTGTTTGATTCCCT
*ica*R	F	CCATTGACGGACTTTACCAG
*ica*R	R	CAAAGCGATGTGCGTAGGA
*fnb*A	F	GAAGATACAAACCCAGGTGG
*fnb*A	R	GACCATTTTCAGTTCCTAAACCAG
*fnb*B	F	GAAGAAGATACAAACCCAGGTGG
*fnb*B	R	GTGACCATTTTCAGTTCCTAAACC
16S rRNA	F	TCGTGTCGTGAGATGTTGGGTTA
16S rRNA	R	GGTTTCGCTGCCCTTTGTATTGT

References

1. E. S. Place, J. H. George, C. K. Williams and M. M. Stevens, *Chemical Society Reviews*, 2009, **38**, 1139-1151.
2. J. Liao, W. Chen, M. Yang, J. Zhou, Z. Wang, Y. Zhou, C. Ning and H. Yuan, *Materials Horizons*, 2018, **5**, 545-552.
3. H. M. A. Kolken, S. Janbaz, S. M. A. Leeflang, K. Lietaert, H. H. Weinans and A. A. Zadpoor, *Materials Horizons*, 2018, **5**, 28-35.
4. W. Zimmerli, A. Trampuz and P. E. Ochsner, *The New England journal of medicine*, 2004, **351**, 1645-1654.
5. R. O. Darouiche, *The New England journal of medicine*, 2004, **350**, 1422-1429.
6. J. W. Costerton, Z. Lewandowski, D. E. Caldwell, D. R. Korber and H. M. Lappin-Scott, *Annual Review of Microbiology*, 1995, **49**, 711-745.
7. J. W. Costerton, P. S. Stewart and E. P. Greenberg, *Science*, 1999, **284**, 1318-1322.
8. D. Davies, *Nat Rev Drug Discov*, 2003, **2**, 114-122.
9. E. M. Hetrick and M. H. Schoenfisch, *Chemical Society Reviews*, 2006, **35**, 780-789.
10. M. Cloutier, D. Mantovani and F. Rosei, *Trends in Biotechnology*, 2015, **33**, 637-652.
11. P. S. Stewart and J. William Costerton, *The Lancet*, 2001, **358**, 135-138.
12. B. Spellberg, J. G. Bartlett and D. N. Gilbert, *New England Journal of Medicine*, 2013, **368**, 299-302.
13. J. H. Yang, P. Bhargava, D. McCloskey, N. Mao, B. O. Palsson and J. J. Collins, *Cell Host & Microbe*, 2017, **22**, 757-765.e753.
14. N. Bhaskaran, C. Quigley, C. Paw, S. Butala, E. Schneider and P. Pandiyan, *Frontiers in Microbiology*, 2018, **9**.

15. S. Kalghatgi, C. S. Spina, J. C. Costello, M. Liesa, J. R. Morones-Ramirez, S. Slomovic, A. Molina, O. S. Shirihai and J. J. Collins, *Science Translational Medicine*, 2013, **5**, 192ra185-192ra185.

16. L. Tan, J. Li, X. Liu, Z. Cui, X. Yang, S. Zhu, Z. Li, X. Yuan, Y. Zheng, K. W. K. Yeung, H. Pan, X. Wang and S. Wu, *Advanced Materials*, 2018, **30**, 1801808.

17. Y. Yu, G. Chen, J. Guo, Y. Liu, J. Ren, T. Kong and Y. Zhao, *Materials Horizons*, 2018, **5**, 1137-1142.

18. J. Haldar, A. K. Weight and A. M. Klibanov, *Nature Protocols*, 2007, **2**, 2412.

19. C. T. O'Loughlin, L. C. Miller, A. Siryaporn, K. Drescher, M. F. Semmelhack and B. L. Bassler, *Proceedings of the National Academy of Sciences*, 2013, **110**, 17981-17986.

20. M. T. Greiner, M. G. Helander, W.-M. Tang, Z.-B. Wang, J. Qiu and Z.-H. Lu, *Nat Mater*, 2012, **11**, 76-81.

21. J. Ng, S. Xu, X. Zhang, H. Y. Yang and D. D. Sun, *Advanced Functional Materials*, 2010, **20**, 4287-4294.

22. J. Wang, J. Li, S. Qian, G. Guo, Q. Wang, J. Tang, H. Shen, X. Liu, X. Zhang and P. K. Chu, *ACS applied materials & interfaces*, 2016, **8**, 11162-11178.

23. H. Tan, Z. Peng, Q. Li, X. Xu, S. Guo and T. Tang, *Biomaterials*, 2012, **33**, 365-377.

24. C. Zhu, H. Tan, T. Cheng, H. Shen, J. Shao, Y. Guo, S. Shi and X. Zhang, *The Journal of surgical research*, 2013, **183**, 204-213.

25. M. Lucke, G. Schmidmaier, S. Sadoni, B. Wildemann, R. Schiller, N. P. Haas and M. Raschke, *Bone*, 2003, **32**, 521-531.

26. G. Guo, H. Zhou, Q. Wang, J. Wang, J. Tan, J. Li, P. Jin and H. Shen, *Nanoscale*, 2017, **9**, 875-892.

27. *U.S. Pat.,* WO200198531-A1.

28. J. A. Kiernan, in *Histological and Histochemical Methods: Theory and Practice* ed. J. A. Kiernan, Pergamon Press, Oxford, 1981, p. 220.

29. K. A. Weber, L. A. Achenbach and J. D. Coates, *Nature Reviews Microbiology*, 2006, **4**, 752.

30. A. J. M. Stams and C. M. Plugge, *Nature Reviews Microbiology*, 2009, **7**, 568.

31. J. Simon, R. J. M. van Spanning and D. J. Richardson, *Biochimica et Biophysica Acta (BBA) - Bioenergetics*, 2008, **1777**, 1480-1490.

32. J. Schirawski and G. Unden, *European Journal of Biochemistry*, 2001, **257**, 210-215.

33. R. K. Thauer, K. Jungermann and K. Decker, *Bacteriological Reviews*, 1977, **41**, 100-180.